

# Doping dependence of magnetic excitations of 1D cuprates as probed by Resonant Inelastic x-ray Scattering

Filomena Forte<sup>1,2</sup>, Mario Cuoco<sup>1,2</sup>, Canio Noce<sup>1,2</sup>, and Jeroen van den Brink<sup>3</sup>

<sup>1</sup>*CNR-SPIN, I-84084 Fisciano (SA), Italy*

<sup>2</sup>*Dipartimento di Fisica “E. R. Caianiello”, Università di Salerno, I-84084 Fisciano (SA), Italy and*

<sup>3</sup>*Institute for Theoretical Solid State Physics, IFW-Dresden, D01171 Dresden, Germany*

(Dated: November 18, 2018)

We study the dynamical, momentum dependent two- and four-spin response functions in doped and undoped 1D cuprates, as probed by resonant inelastic x-ray scattering, using an exact numerical diagonalization procedure. In the undoped  $t - J$  system the four-spin response vanishes at  $\pi$ , whereas the two-spin correlator is peaked around  $\pi/2$ , with generally larger spectral weight. Upon doping spectra tend to soften and broaden, with a transfer of spectral weight towards higher energy. However, the total spectral weight and average peak position of either response are only weakly affected by doping up to a concentration of  $1/8$ . Only the two-spin response at  $\pi$  changes strongly, with a large reduction of spectral weight and enhancement of excitation energy. At other momenta the higher-energy, generic features of the magnetic response are robust against doping. It signals the presence of strong short-range antiferromagnetic correlations, even after doping mobile holes into the system. We expect this to hold also in higher dimensions.

PACS numbers: 78.70.-g 74.72.-h 78.70.Ck 71.27.+a

## I. INTRODUCTION

Cuprate materials have proven a fertile ground for the study of strong electronic correlations and quantum magnetism. Spectroscopic techniques are powerful tools to obtain information about these properties, since they provide direct information on the electronic and magnetic elementary excitations, which are related to the energy spectra, the crystal structure, and so on. Among the spectroscopic techniques used to probe magnetic excitations in cuprates, Resonant Inelastic X-ray Scattering (RIXS) has gained much interest because of the recent increases in energy and momentum resolution, due to the enhanced brilliance of synchrotron x-ray sources and the advances in instrumentations. This has placed RIXS at the forefront in the study of the momentum dependent electronic and magnetic responses over a wide energy range.<sup>1–15</sup>

In the RIXS process, x-ray radiation is inelastically scattered by the matter and the change in energy, momentum and polarization can be related to intrinsic excitations in the material. This process is resonant because the energy of an incoming photon is tuned to match an element absorption edge, thus allowing a large enhancement of the scattered intensity. In this way the x-ray photons can couple to charge, spin and orbital degrees of freedom.<sup>16–30</sup>

In the context of the cuprates, it is by now well-established that RIXS can detect the momentum dependence of charge excitations that are related to the electrons and holes in the  $d$  shell,<sup>2,24,25</sup> but it has also been proved, both experimentally and theoretically, that RIXS is sensitive to the magnetic excitations of cuprates.

## A. Magnetic RIXS in cuprates

In the magnetic sector, RIXS can both create single and double spin flip excitations, corresponding to single- and bi-magnon excitations in ordered Heisenberg antiferromagnets (AFM). Moreover, it has been also predicted that three-magnon scatterings contribute substantially to the magnetic spectral weight,<sup>31</sup> whereas single-magnon excitations were observed in direct RIXS experiments at the Cu L<sub>3</sub> edge on a thin film of La<sub>2</sub>CuO<sub>4</sub>,<sup>19–21,28</sup> and also on small crystals of Sr<sub>2</sub>CuO<sub>2</sub>Cl<sub>2</sub>.<sup>23</sup>

From a theoretical point of view, when the magnetic moment lies in the plane of the  $x^2 - y^2$  orbital, direct spin-flip scattering in cuprates is allowed for symmetry reasons. Thus, at least for this class of materials, L-edge RIXS can be placed on the same footing as neutron scattering, and both are related to the two-spin dynamical correlation function.<sup>19</sup>

At the Cu K-edge, the RIXS process is indirect and single-magnon scattering is forbidden. In this case, magnetic excitations turn out to be due to bi-magnon, as observed in insulating and doped La<sub>2–x</sub>Sr<sub>x</sub>CuO<sub>4</sub> and Nd<sub>2</sub>CuO<sub>4</sub>.<sup>16,22</sup> Subsequently, excitations with a bi-magnon-like dispersion have been observed in cuprates with high-resolution L-edge RIXS,<sup>17,18</sup> and M-edge RIXS.<sup>32</sup> This makes RIXS thus complementary to optical Raman scattering, which also measures the bi-magnon, but only at zero momentum transfer.<sup>33–37</sup>

The microscopic mechanism by which the bi-magnons couple to the intermediate state core-hole in Cu K-edge RIXS is by the core-hole locally modifying the superexchange constant. This leads to the measurement of a four-spin correlation function that can be derived in detail via the Ultrashort Core-hole Lifetime (UCL) expansion.<sup>26,27,38,39</sup> This approach yields a momentum dependence of the cross section in agreement with ex-

periments on undoped cuprates in the Néel state. In particular it reproduces the lack of intensity at  $q=(0,0)$  and  $(\pi,\pi)$ .<sup>16,22</sup> At the Cu L- and M-edges, the coupling mechanism to bi-magnon excitations is similar, resulting in the same cross section to lowest order in the perturbing effective potential between the spin and the core-hole, due to the fact that the superexchange in the intermediate state is, in this case, not just altered but completely blocked locally.<sup>17</sup>

Despite the success in describing undoped cuprates, the doping dependence of both single- and multi-magnon measured by RIXS is rather little unexplored, however with the first data available showing intriguing behavior. For K-edge measurements on  $\text{La}_{2-x}\text{Sr}_x\text{CuO}_4$ , the intensity of the spectral features is found to generally decrease as  $x$  increases.<sup>16,22</sup> The persistence of the highest peak at  $(\pi,0)$ , located around 500 meV, for doping values  $x = 0.07$ , well into the superconducting phase, shows that this excitation survives even if long-range magnetic order is absent, as long as significant short-range magnetic correlations are present, which is well-known to be the case in the superconducting state of LSCO.<sup>40,41</sup> The evolution upon doping observed in L-edge RIXS measurements on LSCO is even more captivating, showing the existence of a high energy “undoped” branch in addition to the lower-energy dispersive features measured in neutron scattering, which can be related to the presence of a stripe liquid<sup>21</sup>.

## B. Aim and Outline

In this paper we analyze the doping dependence of magnetic RIXS in cuprates, and particularly we explore the evolution of the magnetic excitations with doping. We focus on 1D systems because i) strong quantum fluctuations are present, that maximally effect the magnetic ordering, ii) the existence of an exact theoretical results for magnetic excitations in the undoped 1D Heisenberg AFM, formulated in the spinon language, provides a stringent reference test for our numerical spectra, iii) the sampling of the Brillouin Zone (BZ) is much more dense than in the 2D case, and iv) the results are directly relevant for RIXS on 1D cuprates, such as  $\text{Sr}_2\text{CuO}_3$ , where experiments probing the low-energy magnetic excitations are entirely feasible.<sup>42</sup> These 1D spin liquid states may be relevant to the proposed stripe liquid behavior in high-temperature superconductors.

We present numerical calculations of different-time Two-Spin (TS) and Four-Spin (FS) correlation functions, evaluated on 22 sites chain for the Heisenberg model and 16 sites chain for the  $t - J$  model, in the low doping regime with a doping concentration up to  $1/8$ . Even if the analysis is limited by the finite length of the system, one can extract relevant information about the intensity and the dispersion of the magnetic features by quantitative analysis of total spectral weight ( $W_0$ ), and its first moment ( $W_1$ ), corresponding to the average energy peak

position. Besides, the higher energy features are expected to be less affected by finite size effects.

We firstly consider the undoped case assuming a description based on the nearest-neighbour AFM Heisenberg model on a chain. It turns out that both TS and FS correlation functions detect two-spinon excitations, with a spectral weight that is concentrated at the lower boundary of the continuum of excitations. We point out that TS and FS access excitations belonging to orthogonal subspaces, having total spin  $S=1$  and  $S=0$ , respectively. Moreover, we recover crucial differences about momentum dispersion and selection rules: TS is peaked at  $\pi$  where FS vanishes, whereas the latter is peaked at  $\pi/2$ . This result highlights the different length-scale between the TS and the FS excitation. The latter has a characteristic length-scale of  $2a$ , where  $a$  is the lattice spacing, as two (neighboring) exchange bonds are broken in the intermediate state. This shifts the maximum from  $\pi$  towards  $\pm\pi/2$ . These results are consistent with recent Bethe Ansatz calculations<sup>43</sup>. We subsequently study the spectral evolution upon doping, by using the same approach on a  $t - J$  chain containing mobile holes. The magnetic response is found to soften and broaden as a function of the doping concentration. Nevertheless, both the momentum dispersion and the total spectral weight are only slightly affected by a doping of  $1/16$  and  $1/8$ . Only the two-spin response at  $\pi$  changes strongly, with a large reduction of its spectral weight and an enhancement of the excitation energy. At other momenta the higher-energy, generic features of the magnetic response are robust against doping. This shows that the strong short-range antiferromagnetic correlations that are still present after doping give rise to higher energy, damped magnetic excitations with considerable spectral weight.

## II. MAGNETIC EXCITATIONS IN THE 1D $t - J$ MODEL

The  $t - J$  Hamiltonian is one of the most studied model Hamiltonians in the context of high temperature superconductivity in doped, quasi-2D cuprates. Naturally, it is directly relevant to quasi-1D cuprates as well, among which edge-sharing 1D spin chains in  $\text{Li}_2\text{CuO}_2$  and  $\text{GeCuO}_3$  and corner sharing in  $\text{SrCuO}_2$  and  $\text{Sr}_2\text{CuO}_3$ . Charge excitations have been extensively studied by exact diagonalization of Hubbard or charge-transfer models relevant for these systems, also in the context of RIXS<sup>44,45</sup>. In a Hubbard-type model for an undoped chain the presence of singlet excitations of spinon pairs was identified, which is due to the presence of doubly occupied sites<sup>46</sup>. Very recently the RIXS response of the undoped spin-only chain was computed by Bethe Ansatz, which will serve as a benchmark for the present exact diagonalization study.<sup>43</sup> However, the magnetic response of doped  $t - J$  chains has received remarkably little attention in the literature so far. Studies of spin dynamics in the 1D  $t - J$  model have considered the limit

of quarter-filling, with a hole concentration of 3/4, by Monte-Carlo<sup>47,48</sup>, exact-diagonalization<sup>49</sup> and recursion methods<sup>50</sup>, focusing on the regime of weak and strong coupling, comparing one- and two-dimensional features, as well as determining the evolution of the spinon spectrum in presence of magnetic anisotropy. Here we consider the weakly doped chain, with doping concentrations where in the 2D cuprates superconductivity appears and we concentrate on the specific question how far the different types of magnetic excitations to which RIXS is sensitive are affected by the presence of mobile charge carriers.

### A. Zero doping Heisenberg limit

Without doping the 1D  $t - J$  model reduces to the Heisenberg AFM, which is one of the few many-body problems where the ground state, which is a  $SU(2)$  singlet, and the lowest excited states are known exactly.<sup>51</sup> It is described by the Heisenberg Hamiltonian

$$H_{Heis} = J \sum_{\langle i,j \rangle} \mathbf{S}_i \cdot \mathbf{S}_j, \quad (1)$$

where  $J$  is the exchange coupling and  $\mathbf{S}_i$  is the spin operator at the  $i$ -site. It is well-known that this model fails to develop long-range Néel ordering (where neighbouring spins point anti-parallel to each other) even at the lowest temperatures but rather it has an algebraically decaying spin-spin correlation.<sup>52,53</sup> Moreover, the basic excitations are spinons,<sup>54-56</sup> which are topological excitations that can be visualized as twists of  $\pi$  in the spin order. Spinons are fractional particles that possess spin values of  $S = 1/2$ , whose dispersion relation is given by  $e(p) = \pi/2|\sin p|$ ,  $p \in [-\pi, 0]$  in unit of  $J$ . Because of quantum mechanics constraints, only an even number of spinons can be created.

The lowest energy excitations are made of two spinon states, that live within a continuum in  $(k, \omega)$  defined by the kinematic constraints of momentum and energy conservation:  $k = -p_1 - p_2$  and  $\omega = e(p_1) + e(p_2)$ . Hence, for a fixed external momentum, there exists an interval in frequency given by the conditions:

$$\omega \geq \omega_{2,L}(k) = \pi/2|\sin k|; \omega \leq \omega_{2,U}(k) = \pi|\sin k/2|, \quad (2)$$

with  $k \in [0, 2\pi]$ . Here,  $\omega_{2,L}(k)$  and  $\omega_{2,U}(k)$  correspond to the lower and upper bands, respectively. This behavior obviously very different from 2D and 3D systems, where the excitations in the ordered state are spin-waves, which possess a spin value equal to one and follow a well-defined trajectory in energy and wave-vector space in complete contrast to the multi-spinon continuum.

Two-spinon excitations are routinely measured by inelastic neutron scattering<sup>57-60</sup>, but the same response function can also be measured with RIXS. A wealth of theoretical work has been done on the TS correlation

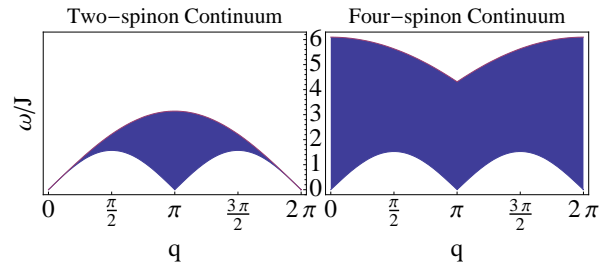


FIG. 1. Two-spinon (left panel) and four-spinon (right panel) continua, stemmed in the colored regions. Color scale is not related to the spectral weight.

function related to neutron structure factor and the exact theoretical spectrum perfectly matches with experimental results.<sup>61-63</sup>

The two-spinon part of the TS function is finite inside the two-spinon continuum, and by construction it vanishes identically outside of it. It has been demonstrated that approximately two thirds of the excitations in this band are indeed of the two-spinon type. The remaining part has a rather small spectral weight and is carried mostly by four-spinon excitations.<sup>64</sup> In Fig.1, these two-spinon and four-spinon bands are schematically represented. Recently it was proven for the FS response function, even if it involves the excitation of two spins, overwhelmingly fractionalizes into two-spinon states.<sup>43</sup>

Within this context, we now start a systematic comparison of the numerical spectra related to the TS and FS correlation functions. We will demonstrate that our results recover the main features (e.g., dispersion and selection rules) of the exact theoretical results, providing the starting point for the subsequent discussion about doping evolution.

### B. Cross section for magnetic RIXS

In the Introduction we mentioned that both direct and indirect RIXS can probe magnetic excitations. In direct RIXS, single spin-flip excitations can be made at the  $2p \rightarrow 3d$  edges of Cu because of the large spin-orbit coupling of the  $2p$  core-hole.<sup>19</sup> Since in the intermediate state spin and orbital angular momentum separately are no longer good quantum numbers, orbital and spin can be exchanged and direct spin-flip processes can in principle be allowed. As in the neutron scattering, the RIXS cross section consists of a local structure factor (depending on the polarization, the experimental geometry and the excitation mechanism) multiplied by the appropriate spin susceptibility<sup>19</sup>

$$S(q, \omega) \propto \sum_f |\langle 0 | S(q) | f \rangle|^2 \delta(\omega - \omega_{fi}), \quad (3)$$

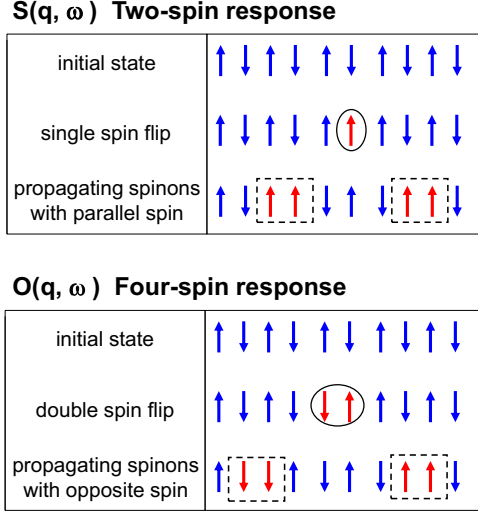


FIG. 2. A schematic picture for a single spin-flip [ $S(q, \omega)$ ] and a double spin-flip [ $O(q, \omega)$ ] in an AFM Heisenberg chain. The first fractionalizes into two-spinon having parallel spins. The latter into two-spinons carrying opposite spin (total spin  $S=0$ ). Spinons are emphasized by the dashed box. The circle indicates the sites where the spin flip process occurs.

where  $|0\rangle$  is the ground state,  $|f\rangle$  an excited state,  $\omega_{fi}$  the energy lost by the photon, and  $S(q) = \sum_i \exp^{iqR_i} \mathbf{S}_{zi}$  is the single-spin form factor. It was shown both theoretically,<sup>19,28</sup> and experimentally<sup>21</sup> that spin-flip excitations are a result of the effect of  $L_z S_z$  operator in the core hole spin-orbit coupling, so one can get a pure spin-flip transition for a  $\text{Cu}^{2+}$  ion with a hole in the  $3d_{x^2-y^2}$  orbital only if the spin is not parallel to the  $z$ -axis.

For indirect RIXS at Cu K-edges ( $1s \rightarrow 4p$ ), the core hole couples to the spin degree of freedom locally modifying the superexchange interactions.<sup>26,27</sup> In this process, the total spin of the valence electrons is conserved, and only excitations with at least two spins flipped (with total  $S_z = 0$ ) are allowed.<sup>16,22</sup> Detailed calculations of the magnetic response functions within the UCL expansion<sup>38,39</sup> demonstrated that the magnetic correlation function, measured by indirect RIXS, is a four-spin correlation one,

$$O(q, \omega) \propto \sum_f |\langle 0 | O(q) | f \rangle|^2 \delta(\omega - \omega_{fi}), \quad (4)$$

where  $O(q) = \sum_i \exp^{iqR_i} (\sum_\delta \mathbf{S}_i \cdot \mathbf{S}_{i+\delta})$  is the two-spin form factor. At the transition metal L-edges, a similar mechanism occurs (in addition to the direct single spin-flip scattering discussed above) because the photo-excited electron in the  $3d$  subshell frustrates the local superexchange bonds.<sup>17</sup>

To calculate  $S(q, \omega)$  and  $O(q, \omega)$ , we apply the Lanczos algorithm to a 22-sites Heisenberg chain and we employ eigenvectors and eigenvalues for the evaluation of the correlation functions as in Eqs. 3-4. In addition, we perform

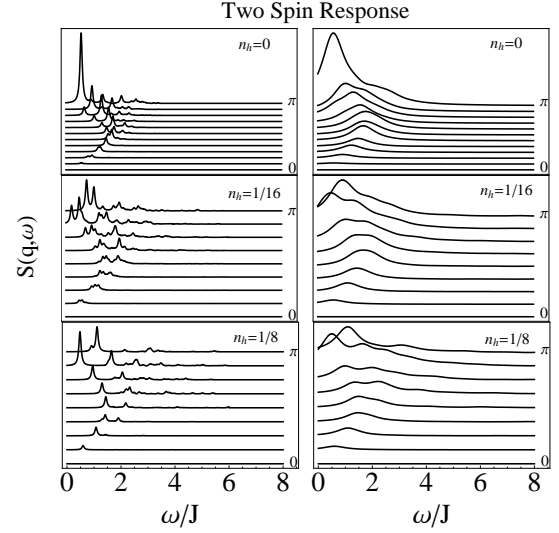


FIG. 3. Inelastic part of  $S(q, \omega)$  at different hole concentration associated to the unequal time correlator defined in Eq. 3, evaluated for a 22-sites Heisenberg chain and 16-sites  $t-J$  chain. For the  $t-J$  model, the hopping is fixed at  $t = 3J$ . The broadening of the lorentzian is  $\gamma = 0.5J(0.05J)$  for the right (left) panel, respectively.

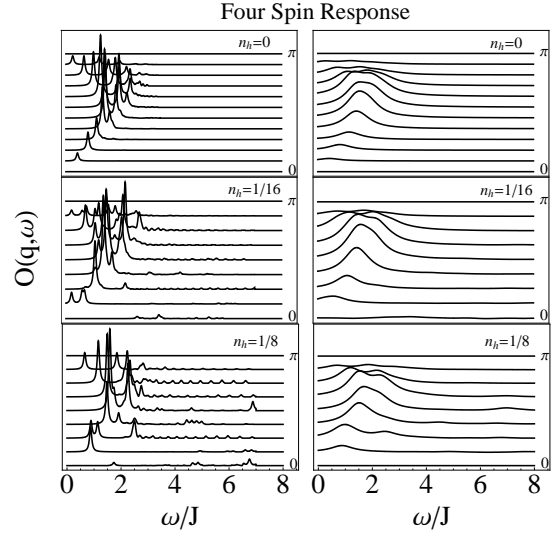


FIG. 4. Inelastic part of  $O(q, \omega)$  at different hole concentration associated to the unequal time correlator defined in Eq. 4, evaluated for a 22-sites Heisenberg chain and 16-sites  $t-J$  chains. For the  $t-J$  model, the hopping is fixed at  $t = 3J$ . The broadening of the lorentzian is  $\gamma = 0.5J(0.05J)$  for the right (left) panel, respectively.

an extensive analysis of the momentum dependence of the frequency moments. We evaluate the average peak position with respect to the double differential cross section  $\frac{d^2\sigma^{(1)}}{d\Omega d\omega}$  as  $W_1 \propto \int \omega \frac{d^2\sigma^{(1)}}{d\Omega d\omega} d\omega$  and we use the total weight  $W_0 \propto \int \frac{d^2\sigma^{(1)}}{d\Omega d\omega} d\omega$  to gain information on the relative ratio as a function of doping concentration and to compare the total intensity of the bare TS and FS spectra. Note that these outcomes are possibly easier to compare with experiments, with respect to the differential cross-section itself. The reason is twofold: i) the presence of statistical errors in experiments is less relevant for the integrated quantities, so a direct comparison with theory is feasible; ii) since lineshapes of the theoretical spectra are typically not Lorentzian, the average excitation energy of the calculated spectra is expected to be the most representative theoretical result.

Before describing the results obtained within our simulation, we would like to point out that the magnetic excitations described by Eqs. 3-4 belong to orthogonal subspaces, as illustrated in Fig.2. The figure aims to clarify that the  $S(q, \omega)$  TS response is related to a single spin-flip that gives rise to a two spinons carrying parallel spin. Instead  $O(q, \omega)$  FS response function is due to a double spin-flip that fractionalize into two spinons, having opposite spin. Starting from the SU(2) singlet ground state, the excitation governing  $S(q, \omega)$  thus carries  $S=1$  while for  $O(q, \omega)$  the excitation has  $S=0$ . This crucial aspect allows to distinguish between ‘polarized’ and ‘unpolarized’ excitations and suggests that the two magnetic responses can have a different sensitivity to for example spinon-spinon interactions or an external magnetic field.

In the top panels of Figs. 3-4, we report the undoped inelastic intensity evaluated numerically starting from TS and FS correlation functions, respectively. There are several common features emerging: the dispersions show similar behavior, the excitation spectrum is mainly located in the two-spinon band, both for  $S(q, \omega)$  and  $O(q, \omega)$ , with an energy scale  $\omega_{2,L} < \omega < \omega_{2,U}$ . Moreover, the intensity is dominated by the spectral weight at the lower threshold of the two-spinon continuum. These results confirm that both  $S(q, \omega)$  and  $O(q, \omega)$  mainly fractionalize in two-spinon excitations<sup>43</sup>. From a closer inspection at the energy region comprised between the upper boundary of the two-spinon continuum and the upper boundary of the four-spinon continuum, high energy tails emerge as consequence of the four-spinon part of the structure factors, that are finite but very small and rapidly approaching to zero.

Nevertheless, spectra do show differences in dispersion. Looking at the white circles of Fig. 5, we infer that for the correlation function  $O(q, \omega)$  the spectrum disperses from zero at  $q = 0$ , up to a maximum of  $\sim 2J$  at  $\pi/2$ , the intensity is suppressed at  $\pi$  and nearby, a fact that is due to structure factor  $e^{iqR_i}$  and not to the density of states, as reported in lower panel of Fig. 5 where the moment  $W_1$  is plotted. The vanishing of the RIXS intensity described by  $O(q, \omega)$  at the antiferromagnetic wavevector  $\pi$  is due to the cancellation of the sums over the two sublattices in

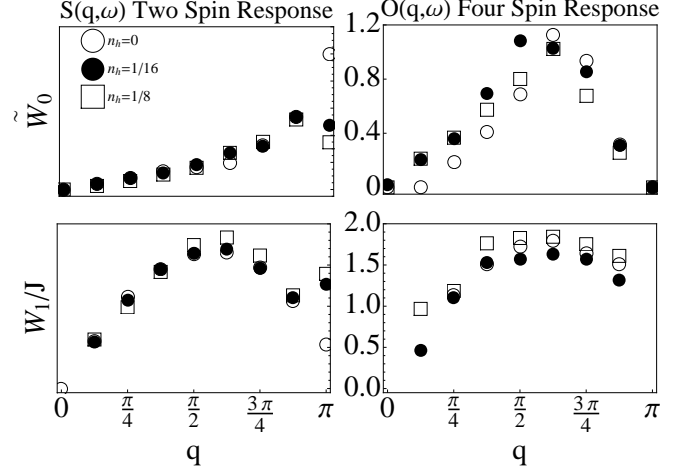


FIG. 5. Total weight (upper panel) and first moment (lower panel) of the TS (left side) and FS (right side) correlation function on a 16-sites chain, for different doping concentrations. For convenience of graphical representation,  $W_0$  is scaled to the total weight at  $\pi$ . Missing points for  $W_1$  are due to vanishing spectral weights.

an antiferromagnetic order. A more detailed explanation can be found in Ref.<sup>27</sup>. On the contrary,  $S(q, \omega)$  has its maximum at  $\pi$  (see Fig. 5). The appearance of a satellite peak at the AFM point located at higher energies can also be noticed. Finally, we remark that, as long as the bare correlation functions are considered, the total weight is larger in the FS case, almost all over the BZ (away from  $\pi$ ), while the highest peak intensities are comparable.

### C. Doping dependence

The doped Heisenberg model is here considered in terms of the single-band  $t - J$  model,<sup>65</sup>

$$H_{t-J} = -t \sum_{\langle i, \delta \rangle, \sigma} \left( \tilde{d}_{i, \sigma}^\dagger \tilde{d}_{i+\delta, \sigma} + h.c. \right) + J \sum_{\langle i, j \rangle} \mathbf{S}_i \cdot \mathbf{S}_j, \quad (5)$$

where the sums run over all the  $\langle i, j \rangle$  bonds, counted once, and  $\tilde{d}$  operators describe electrons in the  $d$  electronic levels with the constraint of no double occupancy.

By following the same procedure described in the previous section, we analyze the evolution upon doping of the TS and FS spectra. Two cases are considered: the hole concentration  $n_h = 1/16$  and  $n_h = 1/8$ , respectively. In Figs. 3 and 4 we report the spectra for  $t/J = 3$ , a ratio that is typical for corner-sharing cuprate perovskites. As one can see, the spectra are generally softened and

broadened and the intensity of the highest peaks is reduced as  $n_h$  is increased. This effect is more dramatic at  $\pi$  for TS, where the peak is strongly damped. In contrast, the doping does not affect substantially the dispersion of the excitation continuum, the only effect being a transfer of spectral weight towards the upper threshold of the two-spinon continuum, with tails in the four-spinon region. Concerning the selection rules, the inelastic intensity is vanishing at  $q = 0$  for both TS and FS, and it is suppressed at  $\pi$  for  $O(q, \omega)$ .

Considering the frequency moments reported in Fig. 5, interesting features come out. Namely, as long as the TS is concerned, major differences occur around the AFM wave-vector, where  $W_0$  strongly decreases with the increases of the doping. This result is somewhat expected since AFM correlations are weakened by doping. The evolution of  $W_1$  suggests that the average peak position stays almost unchanged upon doping; nevertheless it is shifted to  $\omega \sim 2J$  approaching  $\pi$ . As compared to the TS correlation function, the intensity of the FS appears to be renormalized in a less dramatic way. The total weight is even increased in the first half of the BZ (see Fig. 5) and the intensity of the highest peak at  $\pi/2$  is much less softened than the corresponding TS at  $\pi$ . A further look at  $W_1$  allows to conclude that  $n_h=1/16$  leaves the dispersion of the average peak position unmodified while, by increasing  $n_h$ , the dispersion is shifted to slightly higher energies ( $\omega \sim 2.5J$ ). From these outcomes, we can conclude that both the magnetic dispersions mapped by  $S(q, \omega)$  and  $O(q, \omega)$  are quite robust against the doping, as long as the lightly doped regime is considered, and we also infer that the robustness of the two-spinon feature is directly linked to the existence of short-range AFM correlations, irrespective of doping concentration.

Finally, concerning the transfer of spectral weight towards the upper threshold of the two-spinon continuum, we may deduce that it can be related to an ‘itinerancy effect’ due to the fact that the introduction of mobile carriers induces charge fluctuations that couple to spin excitations. We note that an analogue effect is known to be played by correlation energy. For a single-band 1D Hubbard model at half filling, it has been showed that for large values of the on-site repulsion  $U$ , the spin correlations are dominated by virtual hopping processes of electrons and are described in terms of a spin-1/2 Heisenberg chain; in this limit, the spectral weight of spin structure factor  $S(q, \omega)$  is concentrated at the lower spinon

boundary.<sup>66</sup> If  $U$  is decreased, the real hopping of electrons becomes important and eventually dominates the spin response. The electron itinerancy may influence the magnetic correlations, and it is found that the spin structure factor of the Hubbard model differs from the spectrum of the Heisenberg model since a significant spectral weight is concentrated on the upper spinon boundary.<sup>66</sup> We therefore infer that in our case those ‘itinerancy corrections’ arising from charge excitations may be driven by doping with holes, both on TS and FS functions.

### III. CONCLUSIONS

For finite Heisenberg and  $t - J$  chains we have calculated the two-spin (TS) and four-spin (FS) correlation functions, which determine the magnetic RIXS spectra of cuprates. The calculation is performed by means of the Lanczos algorithm applied to 22-sites Heisenberg and 16-sites  $t - J$  models. We firstly show that both functions measure multi-spinon excitations, and we find that the dominant contribution arises from the two-spinon continuum. Depending on which function is considered, one can access to ‘polarized’ ( $S = 1$ ) or ‘unpolarized’ ( $S = 0$ ) excitations, resulting also in a different momentum dispersion. Then, as long as the Heisenberg model is concerned, one observes that  $O(q, \omega)$  peaks at  $\pi/2$  while  $S(q, \omega)$  peaks at  $\pi$ , where  $O(q, \omega)$  vanishes; away from  $\pi$ , the first has a total weight lower than the latter. When doping is introduced, both the TS and FS spectra are softened and spread out. The maximum peak intensities are strongly renormalized, but the total integrated intensity is slightly modified: the spectra tend to broaden. The TS and FS spectra show a general transfer of spectral weight towards the higher energy sectors of the two-spinon band. The main features of the TS and FS spectra, however, exemplified by for instance their zeroth and first moment, show a remarkable robustness against to doping.

### ACKNOWLEDGMENTS

The research leading to these results has received funding from the FP7/2007-2013 under grant agreement N. 264098 - MAMA. We thank A. Klauser and J.-S. Caux for fruitful discussions.

<sup>1</sup> C. -C. Kao, W. A. L. Caliebe, J. B. Hastings, and J. M. Gillet, Phys. Rev. B **54**, 16361 (1996).

<sup>2</sup> J. P. Hill, C.-C. Kao, W. A. L. Caliebe, M. Matsubara, A. Kotani, J. L. Peng, and R. L. Greene, Phys. Rev. Lett. **80**, 4967 (1998).

<sup>3</sup> P. Kuiper, J. H. Guo, C. Sathe, L. C. Duda, J. Nordgren, J. J. M. Poethuizen, F. M. F. de Groot, and G. A. Sawatzky, Phys. Rev. Lett. **80**, 5204 (1998).

<sup>4</sup> P. Abbamonte, C. A. Burns, E. D. Isaacs, P. M. Platzman, L. L. Miller, S. W. Cheong, and M. V. Klein, Phys. Rev. Lett. **83**, 860 (1999).

<sup>5</sup> M. Z. Hasan, E. D. Isaacs, Z. X. Shen, L. L. Miller, K. Tsutsui, T. Tohyama, and S. Maekawa, Science **288**, 1811 (2000).

<sup>6</sup> M. Z. Hasan, P. A. Montano, E. D. Isaacs, Z. X. Shen, H. Eisaki, S. K. Sinha, Z. Islam, N. Motoyama, and S. Uchida,

- Phys. Rev. Lett. **88**, 177403 (2002).
- <sup>7</sup> Y. J. Kim, J. P. Hill, C. A. Burns, S. Wakimoto, R. J. Birgeneau, D. Casa, T. Gog, and C. T. Venkataraman, Phys. Rev. Lett. **89**, 177003 (2002).
  - <sup>8</sup> Y. J. Kim *et al.*, Phys. Rev. Lett. **92**, 137402 (2004).
  - <sup>9</sup> G. Ghiringhelli, N. B. Brookes, E. Annese, H. Berger, C. Dallera, M. Grioni, L. Perfetti, A. Tagliaferri, and L. Braicovich, Phys. Rev. Lett. **92**, 117406 (2004).
  - <sup>10</sup> K. Ishii *et al.*, Phys. Rev. Lett. **94**, 187002 (2005).
  - <sup>11</sup> K. Ishii *et al.*, Phys. Rev. Lett. **94**, 207003 (2005).
  - <sup>12</sup> S. Grenier *et al.*, Phys. Rev. Lett. **94**, 047203 (2005).
  - <sup>13</sup> L. Lu *et al.*, Phys. Rev. Lett. **95**, 217003 (2005).
  - <sup>14</sup> E. Collart, A. Shukla, J.-P. Rueff, P. Leininger, H. Ishii, I. Jarrige, Y. Q. Cai, S.-W. Cheong, and G. Dhalenne, Phys. Rev. Lett. **96**, 157004 (2006).
  - <sup>15</sup> S. Wakimoto *et al.*, Phys. Rev. Lett. **102**, 157001 (2009).
  - <sup>16</sup> J. P. Hill *et al.*, Phys. Rev. Lett. **100**, 097001 (2008).
  - <sup>17</sup> L. Braicovich *et al.*, Phys. Rev. Lett. **102**, 167401 (2009).
  - <sup>18</sup> J. Schlappa *et al.*, Phys. Rev. Lett. **103**, 047401 (2009).
  - <sup>19</sup> L. J. P. Ament, G. Ghiringhelli, M.M. Sala, L. Braicovich, and J. van den Brink, Phys. Rev. Lett. **103**, 117003 (2009).
  - <sup>20</sup> L. Braicovich *et al.*, Phys. Rev. B **81**, 174533 (2010).
  - <sup>21</sup> L. Braicovich *et al.*, Phys. Rev. Lett. **104**, 077002 (2010).
  - <sup>22</sup> D. S. Ellis *et al.*, Phys. Rev. B **81**, 085124 (2010).
  - <sup>23</sup> M. Guarise *et al.*, Phys. Rev. Lett. **105**, 157006 (2010).
  - <sup>24</sup> A. Kotani and S. Shin, Rev. Mod. Phys. **73**, 203 (2001).
  - <sup>25</sup> L. Ament *et al.*, Rev. Mod. Phys. (2011), in press, arXiv:1009.3630.
  - <sup>26</sup> J. van den Brink, Europhys. Lett. **80**, 47003 (2007).
  - <sup>27</sup> F. Forte, L. J. P. Ament, and J. van den Brink, Phys. Rev. B **77**, 134428 (2008).
  - <sup>28</sup> M. W. Haverkort, Phys. Rev. Lett. **105**, 167404 (2010).
  - <sup>29</sup> T. Nagao and J.I. Igarashi, Phys. Rev. B **75**, 214414 (2007).
  - <sup>30</sup> J.I. Igarashi and T. Nagao, arxiv.org/abs/1104.4683.
  - <sup>31</sup> L. J. P. Ament, J. van den Brink, arXiv:1002.3773.
  - <sup>32</sup> B. Freelon *et al.*, arXiv:0806.4432 unpublished.
  - <sup>33</sup> D. Salamon, R. Liu, M. V. Klein, M. A. Karlow, S. L. Cooper, S. W. Cheong, W. C. Lee, and D. M. Ginsberg, Phys. Rev. B **51**, 6617 (1995).
  - <sup>34</sup> G. Blumberg, P. Abbamonte, M. V. Klein, W. C. Lee, D. M. Ginsberg, L. L. Miller, and A. Zibold, Phys. Rev. B **53**, R11930 (1996).
  - <sup>35</sup> J. G. Naeini, X. K. Chen, J. C. Irwin, M. Okuya, T. Kimura, and K. Kishio, Phys. Rev. B **59**, 9642 (1999).
  - <sup>36</sup> S. Sugai and H. Hayamizu, J. Phys. Chem. Solids **62**, 177 (2001).
  - <sup>37</sup> L. H. Machtoub, B. Keimer, and K. Yamada, Phys. Rev. Lett. **94**, 107009 (2005).
  - <sup>38</sup> J. van den Brink and M. van Veenendaal, Europhys. Lett., **73**, 121 (2006).
  - <sup>39</sup> L.J.P. Ament, F. Forte, and J. van den Brink, Phys. Rev. B **75**, 115118 (2007).
  - <sup>40</sup> S. Wakimoto, H. Zhang, K. Yamada, I. Swainson, H. Kim, and R. J. Birgeneau, Phys. Rev. Lett. **92**, 217004 (2004).
  - <sup>41</sup> O. J. Lipscombe, S. M. Hayden, B. Vignolle, D. F. McMorrow, and T. G. Perring, Phys. Rev. Lett. **99**, 067002 (2007).
  - <sup>42</sup> J. W. Seo, K. Yang, D. W. Lee, Y. S. Roh, J. H. Kim, H. Eisaki, H. Ishii, I. Jarrige, Y. Q. Cai, D. L. Feng, and C. Kim, Phys. Rev. B **73**, 161104(R) (2006).
  - <sup>43</sup> A. Klauser, J. Mossel, J.-S. Caux and J. van den Brink, Phys. Rev. Lett. **106**, 157205 (2011).
  - <sup>44</sup> D. Qian, Li Yinwan, M.Z. Hasan, D.M. Casa, T. Gog, Y.-D. Chuang, K. Tsutsui, T. Tohyama, S. Maekawa, H. Eisaki and S. Uchida, J. Phys. Chem. Solids, **66**, 2212, 2005
  - <sup>45</sup> K. Tsutsui, T. Tohyama and S. Maekawa, Phys. Rev. Lett. **91**, 117001 (2003).
  - <sup>46</sup> K. Tsutsui, T. Tohyama and S. Maekawa, Phys. Rev. B. **61**, 7180 (2000).
  - <sup>47</sup> F.F. Assaad and D. Wurtz, Phys. Rev. B **44**, 2681 (1991).
  - <sup>48</sup> J. Deisz, K.H. Luk, M. Jarrell, and D.L. Cox, Phys. Rev. B **46**, 3410 (1992).
  - <sup>49</sup> T. Tohyama, P. Horsch and S. Maekawa, Phys. Rev. Lett. **74**, 980 (1995).
  - <sup>50</sup> S. Zhang, M. Karbach, G. Muller, and J. Stolze, Phys. Rev. B **55**, 6491 (1997).
  - <sup>51</sup> H. Bethe, Z. Phys. **71**, 205 (1931).
  - <sup>52</sup> A. Luther and I. Peschel, Phys. Rev. B **12**, 3908 (1975).
  - <sup>53</sup> H. Q. Lin and D. K. Campbell, J. Appl. Phys. **69**, 5947 (1991).
  - <sup>54</sup> L. D. Faddeev and L. A. Takhtadjan, Phys. Lett. A **85**, 375 (1981).
  - <sup>55</sup> M. Fowler, and M.W. Puga, Phys. Rev. B **18** 421 (1978).
  - <sup>56</sup> P. W. Anderson, Science **235** 1196 (1987).
  - <sup>57</sup> M. Kenzelmann, R. Coldea, D. A. Tennant, D. Visser, M. Hofmann, P. Smeibidl and Z. Tylczynski, Phys. Rev. B **65**, 144432 (2002).
  - <sup>58</sup> M. B. Stone, D. H. Reich, C. Broholm, K. Lefmann, C. Rischel, C. P. Landee and M. M. Turnbull, Phys. Rev. Lett. **91**, 037205 (2003).
  - <sup>59</sup> I. A. Zaliznyak, H. Woo, T. G. Perring, C. L. Broholm, C. D. Frost and H. Takagi, Phys. Rev. Lett. **93**, 087202 (2004).
  - <sup>60</sup> B. Lake, D. A. Tennant, C. D. Frost and S. E. Nagler, Nat. Mater. **4**, 329 (2005).
  - <sup>61</sup> M. Kohno, O. A. Starykh, and L. Balents, Nat. Phys. **3**, 790 (2007).
  - <sup>62</sup> A. C. Walters *et al.*, Nature Physics **5**, 867 (2009).
  - <sup>63</sup> B. Thielemann *et al.*, Phys. Rev. Lett. **102**, 107204 (2009).
  - <sup>64</sup> J. -S. Caux and R. Hagemans, Journal of Statistical Mechanics: Theory and Experiment, P12013 (2006).
  - <sup>65</sup> F. C. Zhang and T. M. Rice, Phys. Rev. B **37**, 3759 (1988).
  - <sup>66</sup> M. J. Bhaseen, F.H.L. Essler, A. Grage, Phys. Rev. B **71**, 020405 (2005).